Original Article
Food Science and Technology
ISSN 0101-2061 (Print)
ISSN 1678-457X (Online)
DOI: https://doi.org/10.5327/fst.576

Optimization and Statistical Modeling of the Adsorptive Capacity of Activated Carbon from Elephant Grass

Regiani Crystina Barbazelli, Marcelo Mendes Pedroza, Daniel Assumpção Bertuol, Magale Karine Diel Rambo

Abstract

With high productivity and easy adaptation to diverse ecosystems, elephant grass (*Pennisetum purpureum* Schum) shows strong potential for biomass production. The aim of this study was to evaluate the efficiency and adsorptive capacity of activated carbon derived from elephant grass, applying the Plackett–Burman methodology to analyze the methylene blue adsorption test. The independent variables considered include temperature (20, 25, and 30 °C), carbon mass (0.3, 0.6, and 0.9 g), solution pH (6.5, 7.5, and 8.5), adsorption time (7, 14, and 21 min), dye concentration (20, 60, and 100 mg/L^{-1}), agitation speed (71, 119, and 167 rpm), and carbon particle diameter (0.45, 1.23, and 2 mm). The experimental responses for dye removal efficiency were all above 98.91%, with a maximum adsorption capacity of 9.99 mg/g, indicating its potential for dye removal. Response surface methodology was employed to optimize the adsorption process, yielding a statistical model with a coefficient of determination (R^2) of 99.4%. The yield of the adsorbent material was approximately 30% of the dry matter. These findings highlight the potential of elephant grass as a sustainable source for producing adsorbents.

Keywords: biomass; elephant grass; activated carbon; adsorbent; statistical modeling; optimization.

Practical Application: Activated charcoal has several practical applications in both medicine and industry. In the medical field, it is used to detoxify cases of poisoning and in the treatment of wounds. In industry, it plays a crucial role in the purification of water, gases, and food. Among its most common uses are incorporation into household water filters, face masks, and as an adsorbent for the removal of odors and impurities in industrial and beverage production processes.

1 INTRODUCTION

Elephant grass (*Pennisetum purpureum* Schum) stands out for its resistance, adapting to adverse conditions such as high temperatures and low availability of water, nitrogen, or carbon dioxide (Barbazelli et al., 2025; Silveira Junior et al., 2022). The grass can be harvested up to four times a year, and it provides a high biomass yield, producing between 25 and 35 oven-dry tons per hectare annually (Flores et al., 2013; Samson et al., 2005). Furthermore, elephant grass biochar is effective in removing nitrate ions, making it a viable option for water decontamination (Adesemuyi et al., 2020).

Activated carbons are fundamental in the food industry, ensuring the quality and safety of products through the adsorption of impurities, odors, and contaminants. However, despite its remarkable adsorption capacity, attributed to its high porosity and wide surface area, activated carbon is associated with high investment costs. This has encouraged the search for low-cost alternative materials that can enhance their effectiveness, as indicated by Pedroza et al. (2023). To evaluate the adsorption capacity of elephant grass biochar and its effectiveness in removing methylene blue (MB) dye, an experiment was conducted (Gregor et al., 2024) to identify the independent variables that most significantly impact the quality of the produced biochar. The central composite face-centered design (CCF) was applied to determine the optimal operating ranges for each process variable (Mateus et al., 2001; Pessoti et al., 2020).

1.1 Relevance of the work

The importance of elephant grass activated carbon in adsorption stems from its vast internal surface area and high porosity, characteristics that make it a highly effective adsorbent in the removal of a wide variety of impurities. This includes organic molecules, contaminants, and substances responsible for odor, taste, and color in media such as water. Such adsorption capacity gives elephant grass activated carbon versatility, low cost, and sustainability, making it essential in treatment and purification processes.

Received Oct. 9, 2025.
Accepted Oct. 21, 2025.
[1]*Universidade Federal do Tocantins, Graduate Program in Environmental Sciences, Tocantins, Brazil.*
[2]*Instituto Federal do Tocantins, Department of Electrical Engineering, Palmas, Tocantins, Brazil.*
[3]*Universidade Federal de Santa Maria, Department of Chemical Engineering, Santa Maria, Rio Grande do Sul, Brazil.*
*Corresponding author: regiani@mail.uft.edu.br
Conflict of interest: nothing to declare.
Funding: nothing to declare.

2 MATERIAL AND METHODS

2.1 Biomass preparation

Samples of elephant grass (*P. purpureum* Schum) BRS Capiaçu were collected from the experimental unit of EMBRAPA Fisheries and Aquaculture in Tocantins, approximately 180 days after planting. After collection, the material was oven-dried at 85 °C for 72 hours and stored in containers for subsequent analysis.

2.2 Mass loss kinetics

The experiments were carried out in a drying oven, model SL-100, at a temperature of 50 °C. The biomass was heated in a porcelain crucible. The heating times adopted in this study were 1, 2, 3, 5, 6, and 7 hours. After heating for a given time interval, the crucible was cooled in a desiccator and weighed on an analytical balance. Following the mass loss kinetics procedures, the mass loss rate was calculated in mg/g*h (Pedroza et al., 2021).

2.3 Biomass pyrolysis process and charcoal yield

The thermal conversion was carried out in a fixed-bed stainless steel reactor measuring 60 cm in length and 5.0 cm in external diameter. The reactor was heated by a reclining split furnace (FLYEVER brand, model FE50RPN, line 05/50) and operated in batch mode. The inert carrier gas used in the reaction was steam, heated to 133 °C in an autoclave at a pressure of 2 kgf/cm^2. The pyrolysis of the material was carried out in four experiments: (a) temperature of 400 °C with a heating rate of 20 °C/min, (b) temperature of 400 °C with a heating rate of 30 °C/min, (c) temperature of 500 °C with a heating rate of 20 °C/min, and (d) temperature of 500 °C with a heating rate of 30 °C/min. Subsequently, the material was activated at 600 °C.

2.4 Brunauer, Emmett and Teller surface area analysis

A 0.5 g sample of biochar of experiment (a), prepared at an initial temperature of 400 °C with a heating rate of 20 °C/min and subsequently activated at 600 °C, was subjected to surface area and porosimetry system analysis using a Micromeritics ASAP 2010 instrument to determine the specific N_2-BET surface area and pore size distribution. The standard diameter range used was 0.35–300 nm for pores and 0.01–3.000 m^2/g for surface area. The treatment temperature ranged from 30 to 350 °C.

2.5 Adsorption capacity and dye removal efficiency

In the experiments, the charcoal from experiment (a) was used. The aqueous solution applied in the adsorption test was the cationic dye MB. In all tests, a standard volume of 30 mL of solution was used, with the samples placed on an orbital shaker table (Shaker TE 141), and the adsorption time adopted according to the experimental designs. After the adsorption test, the samples were filtered through analytical paper, and the resulting absorbance was determined using a double-beam spectrophotometer (PERKIN ELMER, LAMBDA 750) at 650 nm.

2.6 Statistical analysis: Experimental design—Plackett–Burman

An experimental design was carried out to examine the effects of seven independent variables, or factors, on the MB dye adsorption test, as presented in Table 1. This analysis was conducted using a variable screening design.

An experimental design was applied using the Plackett–Burman (PB) matrix (Plackett & Burman, 1946; Rodrigues & Iemma, 2014), with 12 tests and 3 replications at the central point, totaling 15 experiments. The following responses were considered in this experimental design: (a) removal efficiency (%) and (b) adsorption capacity or ratio (mg/g).

2.7 Optimization design—Central composite face-centered design

In the optimization design (CCF), the two independent variables that had the greatest effects in the PB design, adsorbent mass and dye concentration, were applied to the adsorption test. The other five variables that did not show significant effects in the PB design were kept constant in this new design: (a) temperature at 20 °C, (b) dye solution pH at 7.5, (c) adsorption time of 7 min, (d) agitation speed of 71 rpm, and (e) activated carbon particle diameter of 0.45 mm.

The experimental matrix and result analysis were performed using Protimiza Experimental Design Software (Plackett & Burman, 1946; Rodrigues & Iemma, 2014). The models produced were validated through analysis of variance (ANOVA) and found to be reliable at a 95% confidence level ($p < .05$). The response surface methodology applied statistical models to predict adjustment experiments and determine the optimal value of the response variables. The independent variables used in this study and their respective levels employed in the optimization design (CCF) were carbon mass (x_1) with levels of 0.3, 0.6, 0.9 g and MB concentration (x_2) with levels of 20, 60, 100 mg/L.

3 RESULTS AND DISCUSSION

3.1 Mass loss kinetics

The raw material was subjected to a kinetic mass loss analysis in an oven at 50 °C. Based on the experimental data, a linear increase in material loss was observed during the first hours of drying. It was estimated that the maximum point of mass loss

Table 1. Independent variables used in this study and their respective levels employed in the experimental design of the adsorption tests.

Factors	Units	Levels		
		(–1)	0	(+1)
Temperature (x_1)	°C	20	25	30
Carbon mass (x_2)	g	0.3	0.6	0.9
Solution pH (x_3)	(–)	6.5	7.5	8.5
Adsorption time (x_4)	min	7	14	21
Dye concentration (x_5)	mg/L	20	60	100
Agitation speed (x_6)	rpm	71	119	167
Activated carbon particle diameter (x_7)	mm	0.45	1.23	2

Source: Author, 2025.

occurred at 5.9 hours, and was 37%. The reduction of water content in the biomass is essential for performing pyrolysis, as it decreases the activation energy required for the reactions occurring during the process. As indicated by Pedroza et al. (2021), during the first hours of the experiments, residues generally lose almost 50% of their initial mass, and after 20 hours the samples contain less than 50% of the original material. This shows that elephant grass has an advantage in terms of mass loss, retaining 63% of the starting material and stabilizing after 5.9 hours, which demonstrates the potential of this biomass for pyrolysis.

3.2 Yield of activated carbon from Elephant Grass

In the study by Irfan et al. (2016), the pyrolysis of halophyte grass (*Achnatherum splendens* L.) at 700 °C resulted in a biochar yield of 24% relative to dry matter. The reduction in biochar yield was attributed to the thermal degradation of cellulose, hemicellulose, and lignin into syngas and bio-oil at the high pyrolysis temperature. In contrast, Ferreira et al. (2019), who investigated the agronomic potential of biochar produced from elephant grass (*P. purpureum* Schum) biomass pyrolyzed at 600 °C, reported a biochar yield of 25.6% by weight. It is well established that pyrolysis conditions and the type of reactor employed are key factors influencing both the yield and quality of biochar.

The pyrolysis conditions evaluated in this study did not significantly affect biochar yield, which ranged from 28.9 to 30.5%, resulting in an average yield of 30% relative to dry matter. This value is higher than those reported by Irfan et al. (2016) and Ferreira et al. (2019), demonstrating its potential for biochar production. Considering the average yield of the activated carbons in this study and analyzing the mass loss of elephant grass, it can be concluded that one metric ton of fresh elephant grass would produce approximately 189 kg of activated carbon, as illustrated in Figure 1.

3.3 Brunauer, Emmett and Teller surface area analysis

Table 2 presents the porosity results of elephant grass biochar analyzed in this study, comparing them with elephant grass biomass from the previous study by Barbazelli et al. (2025). A sixfold increase in Brunauer, Emmett and Teller (BET) surface area, a fivefold increase in Langmuir surface area, and nearly a fivefold increase in pore volume were observed for biochar compared to the original elephant grass, highlighting the potential of biochar. Based on the results shown in Table 3, there is a predominance of mesopores (with sizes between 2 and 50 nm), although there is a trend toward micropores (smaller than 2 nm), as defined by IUPAC (International Union of Pure and Applied Chemistry).

In the study by Irfan et al. (2016), the BET surface area of the raw material, halophyte grass, was 2.01 m^2/g, while the biochar produced at 700 °C exhibited a BET surface area of 5.24 m^2/g. These results highlight the superiority of the biochar produced in the present work as an adsorbent compared to the raw biomass.

Chun et al. (2004) reported that the surface area of biochar produced at 600 °C is greater than that of biochar produced at 700 °C, suggesting that the fine pore structure may be damaged at higher temperatures. According to Ain et al. (2021), biochar from *Parthenium hysterophorus* produced at different pyrolysis temperatures of 300, 450, and 600 °C showed an increase in surface area as the pyrolysis temperature rose from 300 °C to 600 °C, increasing from 0.25 m^2/g to 0.70 m^2/g, along with an increase in the total pore volume from 1.96×10^{-3} cm^3/g to 4.62×10^{-3} cm^3/g. This increase may be attributed to the progressive degradation of hemicellulose, cellulose, and lignin, as well as the formation of channel-like structures during pyrolysis. Irfan et al. (2016) also reported an increase in pore volume from 0.85 to 1.44 m^2/g with the rise in pyrolysis temperature from 300 °C to 700 °C in biochar prepared from a halophyte. Imam and Capareda (2012) observed that high pyrolysis temperatures cause extensive devolatilization of the material, resulting in the generation of

Table 2. Results and comparison between elephant grass biomass and biochar.

Components	Biochar[a]	Biomass[b]
BET surface area ($m^2\ g^{-1}$)	7.48	1.19
Langmuir surface area ($m^2\ g^{-1}$)	9.92	1.85
Micropore area ($m^2\ g^{-1}$)	4.17	
Pore volume ($cm^3\ g^{-1}$)	0.0089	0.0019
Micropore volume ($cm^3\ g^{-1}$)	0.0019	
Pore size (nm)	4.84	6.35

Source: [a]Organized by the authors (2025); [b]Barbazelli et al. (2025).
BET: Brunauer, Emmett and Teller.

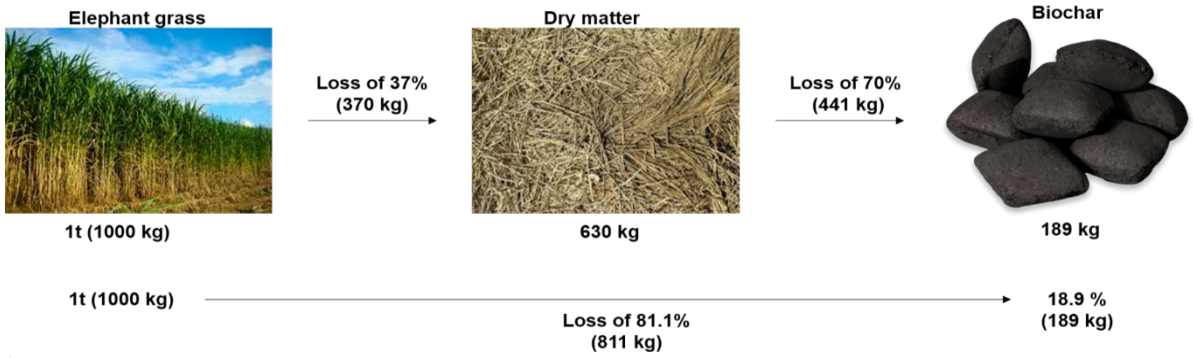

Source: Author, 2025.

Figure 1. Estimated yield of activated carbon from elephant grass.

additional pore volume and higher surface area in the sample, accompanied by enhanced adsorption activity.

3.4 Statistical analysis: Experimental design—Plackett–Burman

The experimental design responses (Table 3) for dye removal efficiency (Y_1) were all above 98.91%, reaching a maximum value of 99.90% in experiment 9. The experiments that demonstrated the highest adsorption capacity (Y_2) were associated with higher dye concentration (100 mg/L) and lower amounts of activated carbon (0.3 g). These conditions were observed in experiments 8, 9, and 10, which removed the largest amount of dye per unit mass of adsorbent, achieving 9.99 mg/g.

In the study by Irfan et al. (2016), the pyrolysis of halophyte grass (*A. splendens* L.) was conducted at three different temperatures (300, 500, and 700 °C), resulting in MB adsorption capacities of 2.35, 2.61, and 2.60 mg/g for the biochars produced at these temperatures, respectively. The biochar samples exhibited nearly similar MB adsorption capacities, indicating that pyrolysis temperature did not significantly influence this property. In contrast, the elephant grass biochar from the present study, in experiments 8, 9, and 10, demonstrated an adsorption capacity (Y_2) of 9.99 mg/g, far exceeding the values reported by Irfan et al. (2016), highlighting the potential of the biochar investigated in this work. The MB adsorption capacities were positively correlated with cation exchange capacity, indicating electrostatic interactions between the biochar surface and MB (Güleç et al., 2022; Irfan et al., 2016; Wang et al., 2023).

When analyzing the MB adsorption capacity of raw elephant grass material, a value of 2.9 mg/g was found, very close to the 2.8 mg/g reported by Irfan et al. (2016). Mustapha et al. (2023) also investigated the adsorption capacity of raw elephant grass under different conditions, observing adsorption kinetics ranging from 2.028 to 3.356 mg/g, with the pseudo-second-order equation providing an excellent fit to the experimental data on MB adsorption, as evidenced by high linear regression coefficient (R^2) values. These findings are consistent with other studies, such as those by Ghosh et al. (2019), Jawad et al. (2018), and Uddin et al. (2017). The results of experiments 8, 9, and 10 (adsorption capacity (Y_2) of 9.99 mg/g) confirm that elephant grass biochar has a superior adsorption potential compared to the raw material. This is attributed to its high specific surface area and the presence of a highly porous structure.

In the analysis of removal efficiency (Y_1), the dye concentration emerged as the only factor with statistical significance in the test (Table 4). With a positive effect of 0.6 (p = .0007), the results indicate that increasing dye concentration enhances the removal of this chemical species during the adsorption process. Since the other variables did not show statistical significance at the 95% confidence level, it is possible to operate within any range of these variables, aiming to optimize process costs and time. In the evaluation of adsorption capacity (Y_2), among the factors analyzed, activated carbon mass (x_2) and dye concentration (x_5) were the only factors with p-values lower than .0015 (Table 4). The other factors showed p-values above the significance level of 0.05. The effect of dye concentration was positive, with a value of 5.3, indicating that the transition from the lowest (–) to the highest (+) level within this design promoted an increase in the adsorption capacity of the carbon. On the other hand, the carbon mass factor showed a negative effect of –4, suggesting that increasing the mass of carbon used in the adsorption test resulted in a reduced adsorption capacity for the dye examined.

The data obtained from the experimental design of the MB adsorption test revealed that the variables temperature, solution pH, adsorption time, agitation speed, and activated carbon particle diameter did not show statistical significance

Table 3. Plackett–Burman design results—methylene blue adsorption tests.

Tests	x_1	x_2	x_3	x_4	x_5	x_6	x_7	Y_1	Y_2
	°C	g	(-)	min	mg/L	rpm	mm	%	mg/g
1	30	0.3	8.5	7	20	71	2	99.46	1.99
2	30	0.9	6.5	21	20	71	0.45	99.40	0.66
3	20	0.9	8.5	7	100	71	0.45	99.90	3.33
4	30	0.3	8.5	21	20	167	0.45	99.06	1.98
5	30	0.9	6.5	21	100	71	2	99.83	3.33
6	30	0.9	8.5	7	100	167	0.45	99.81	3.33
7	20	0.9	8.5	21	20	167	2	98.91	0.66
8	20	0.3	8.5	21	100	71	2	99.87	9.99
9	20	0.3	6.5	21	100	167	0.45	99.90	9.99
10	30	0.3	6.5	7	100	167	2	99.87	9.99
11	20	0.9	6.5	7	20	167	2	99.51	0.66
12	20	0.3	6.5	7	20	71	0.45	99.25	1.98
13	25	0.6	7.5	14	60	119	1.225	99.66	2.99
14	25	0.6	7.5	14	60	119	1.225	99.78	2.99
15	25	0.6	7.5	14	60	119	1.225	99.80	2.99

Variables: (x_1) temperature, (x_2) activated carbon mass, (x_3) solution pH, (x_4) adsorption time, (x_5) dye concentration, (x_6) agitation speed, (x_7) activated carbon particle diameter; Design responses: (Y_1) removal efficiency and (Y_2) adsorption capacity.
Source: Author, 2025.

with respect to dye removal efficiency or adsorption capacity. Therefore, to optimize the process and reduce both cost and processing time, the test was conducted using lower agitation speeds and a shorter adsorption time.

3.5 Optimization Design— Central composite face-centered design

Table 5 details the factor levels used and the 11 experiments conducted, highlighting the responses in terms of removal efficiency and adsorption capacity. The results obtained for removal efficiency (Y_1) were higher than 88.35%, indicating the potential of this biochar as an adsorbent for chemical dyes. Meanwhile, adsorption capacity (Y_2) ranged from 0.61 to 9.6 mg/g.

The statistical models of the design responses, Equation 1 and 2, describe the relationship between the factors influencing removal efficiency (Y_1) and adsorption capacity (Y_2) within the studied range. Removal efficiency (Y_1) showed a calculated *F*-value (F_{cal}) of 11.3 and a tabulated *F*-value (F_{tab}) of 4.46, with the generated linear model (Y_1) presenting a coefficient of determination (R^2) of 74%. As for maximum adsorption capacity (Y_2), the calculated *F*-value (F_{cal}) was 233.6 and the tabulated *F*-value (F_{tab}) was 4.53, with the generated linear model (Y_2) presenting a coefficient of determination (R^2) of 99.4%.

$$Y_1 = 97.02 + 2.86\, x_2 - 2.53\, x_2^2 \quad (1)$$

and

$$Y_2 = 2.91 - 1.92\, x_1 + 0.95\, x_1^2 + 2.40\, x_2 - 1.27\, x_1 x_2 \quad (2)$$

In these models, a positive sign (+) indicates a positive effect, while a negative sign (–) indicates a negative effect. It is evident that dye concentration (x_2) has a positive influence on the amount adsorbed, meaning that as dye concentration increases, higher values are observed for both Y_1 and Y_2. For both removal efficiency (Y_1) and maximum adsorption capacity (Y_2), the calculated *F*-values (F_{cal}) were higher than the tabulated *F*-values (F_{tab}), suggesting that the

Table 4. Regression coefficients for removal efficiency (%) and adsorption capacity (mg/g) in the methylene blue test.

Factors	–1	0	1	Y_1 Removal efficiency (%)		Y_2 Adsorption capacity (mg/g)	
				Effect	*p*-value	Effect	*p*-value
Mean				99.6	0	4	0
Curvature				0.4	.1351	–2	.2641
Temperature (x_1)	20	25	30	0	.8792	–0.9	.2674
Carbon mass (x_2)	0.3	0.6	0.9	0	.9326	–4	.0015
Solution pH (x_3)	6.5	7.5	8.5	–0.1	.2344	–0.9	.2674
Adsorption time (x_4)	7	14	21	–0.1	.1938	0.9	.2674
Dye concentration (x_5)	20	60	100	0.6	.0007	5.3	.0003
Agitation speed (x_6)	71	119	167	–0.1	.2956	0.9	.2674
Particle diameter (x_7)	0.45	1.225	2	0	.8264	0.9	.2658

$p < .05$ (95%CI). Y_1: removal efficiency; Y_2: adsorption capacity.
Source: Author, 2025.

Table 5. Central composite face-centered design results—methylene blue adsorption test.

Tests	x_1	x_2	x_1—Carbon mass	x_2—Methylene blue concentration	Y_1—Removal efficiency	Y_2—Adsorption capacity
			g	mg/L	%	mg/g
1	–1	–1	0.3	20	94.54	1.89
2	1	–1	0.9	20	92.00	0.61
3	–1	1	0.3	100	96.00	9.60
4	1	1	0.9	100	97.37	3.25
5	–1	0	0.3	60	97.51	5.85
6	1	0	0.9	60	96.62	1.93
7	0	–1	0.6	20	88.35	0.88
8	0	1	0.6	100	98.71	4.94
9	0	0	0.6	60	97.33	2.92
10	0	0	0.6	60	96.86	2.91
11	0	0	0.6	60	96.79	2.90

minimum and maximum.
Source: Author, 2025.

models are statistically significant with respect to the accuracy of the results. The linear model generated for Y_2 presented a coefficient of determination (R^2) of 99.4%, demonstrating that the regression model has an excellent fit and is highly reliable.

The MB concentration variable (x_2) has a significant influence on removal efficiency (Y_1). This indicates that increasing dye concentration leads to greater removal of this chemical species during the adsorption process. Through optimization, the ideal experimental conditions were identified to maximize removal efficiency using elephant grass biochar: (a) fixing the adsorbent mass at 0.6 g and (b) adjusting dye concentration to 84 mg/L.

The Pareto diagram presented in Figure 2A illustrates the significant effect of the variables carbon mass (x_1) and dye concentration (x_2) on adsorption capacity (Y_2), showing that these variables exert a substantial influence on the adsorption potential of the activated carbon. The response surface analysis of biochar adsorption capacity, with respect to carbon mass and MB dye concentration, as shown in Figure 2B, revealed that maximum adsorption capacity is achieved at low levels of carbon mass and high dye concentrations. Through optimization using response surface methodology (RSM), the ideal experimental conditions for the adsorption capacity of elephant grass biochar were established. The maximum adsorption capacity values were obtained under the following conditions: (a) adsorbent mass ranging from 0.3 to 0.6 g and (b) dye concentration between 60 and 100 mg/L, as highlighted in the red region of the surface.

As observed, an increase in MB concentration results in a higher adsorption capacity, whereas as the carbon mass increases, the adsorption capacity of the biochar decreases. Notably, adsorption capacity and carbon mass exhibit opposite trends, suggesting that careful control of operational parameters in biochar production is necessary to achieve the optimal quality of the product. According to Mustapha et al. (2023), adsorption capacity increases with the increment of adsorbate concentration at a contact time of 30 minutes. This can be attributed to the increase in the total surface area available for mass transfer and the greater availability of adsorption sites. Throughout the adsorption reaction, the adsorption sites remained unsaturated, which may be explained by the aggregation of adsorbent particles at higher concentrations. Such aggregation would lead to a reduction in the total surface area available for dye adsorption and to an increase in the diffusion path length (Doğan et al., 2009; Mustapha et al., 2023).

This is supported by Yusof et al. (2020), who observed that when more adsorbent is added to a solution, the initial removal capacity increases due to the greater number of available "active sites." However, there is a point at which adding more adsorbent no longer improves removal efficiency. Thus, once a specific amount of adsorbent is reached, the removal rate stabilizes (Souza Borges et al., 2025; Yusof et al., 2020). Therefore, determining the optimal biochar dosage is a crucial aspect in experimental studies. The use of CCF as a statistical tool made it possible to determine the optimized condition for the decision-making process.

4 CONCLUSIONS

The results of this study show that elephant grass activated charcoal can be considered an economically and environmentally sustainable option for dye removal, due to its high productivity, low cost, and high adsorptive capacity comparable to commercial activated carbon.

In the experimental design, MB concentration and carbon mass were identified as significant variables in biomass pyrolysis. Dye removal efficiencies (Y_1) exceeded 98.91, reaching up to 99.90%. The maximum adsorption capacity (Y_2) was approximately 9.99 mg/g, underscoring its effectiveness in dye removal. The study also employed the CCF, and the statistical model generated presented a coefficient of determination (R^2) of 99.4%, highlighting its accuracy and reliability in predicting maximum adsorption capacity. The optimal experimental conditions determined by RSM were: (a) adsorbent mass between 0.3 and 0.6 g and (b) dye concentration between 60 and 100 mg/L, resulting in a maximum adsorption capacity of 9.60 mg/g.

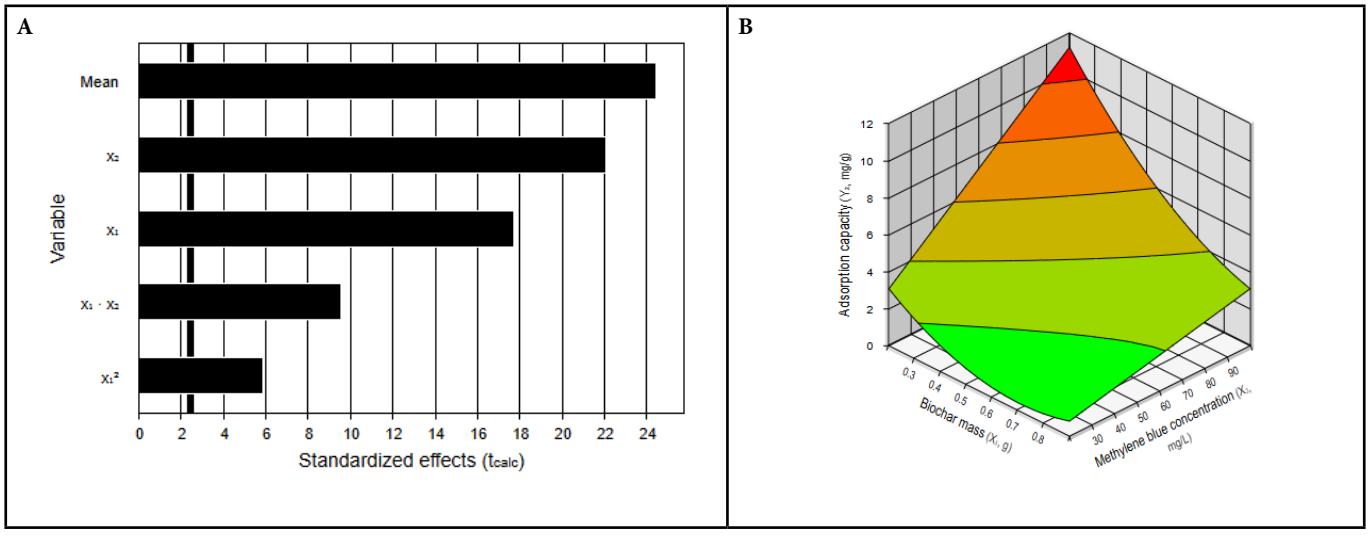

Source: Author, 2025.

Figure 2. **(A)** Pareto diagram of adsorption capacity, **(B)** response surfaces for adsorption capacity.

REFERENCES

Adesemuyi, M. F., Adebayo, M. A., Akinola, A. O., Olasehinde, E. F., Adewole, K. A., & Lajide, L. (2020). Preparation and characterisation of biochars from elephant grass and their utilisation for aqueous nitrate removal: Effect of pyrolysis temperature. *Journal of Environmental Chemical Engineering*, *8*(6), Article 104507. https://doi.org/10.1016/J.JECE.2020.104507

Ain, Q., Shafiq, M., Capareda, S. C., Firdaus-e-Bahrain. (2021). Effect of different temperatures on the properties of pyrolysis products of Parthenium hysterophorus. *Journal of the Saudi Chemical Society*, *25*(3) Article 101197. https://doi.org/10.1016/j.jscs.2021.101197

Barbazelli, R. C., Rambo, M. K. D, Rambo, M. M. C., Vital, M. K. G. S., Pimentel, T. F., Santos, G. R., Guarda, P. M., & Marto, V. C. O. (2025). Sustainable petrochemical plataform from Elephant Grass. *Ciência e Natura*, *47*, Article e86488. https://doi.org/10.5902/2179460X86488

Chun, Y., Sheng, G., Chiou, C. T., & Xing. B. (2004). Compositions and Sorptive Properties of Crop Residue-Derived Chars. *Environmental Science Technology*, *38*(17), 4649–4655. https://doi.org/10.1021/es035034w

Doğan, M., Harun, A., & Mahir, A. (2009). Adsorption of methylene blue onto hazelnut shell: Kinetics, mechanism and activation parameters. *Journal of Hazardous Materials*, *164*(1), 172–181. https://doi:10.1016/j.jhazmat.2008.07.155

Ferreira, S. D., Manera, C., Silvestre, W. P., Pauletti, G. F., Altafani, R., & Godinho, M. (2019). Use of biochar produced from elephant grass by pyrolysis in a screw reactor as a soil amendment. *Waste Biomass Value*, *10*, 3089–3100. https://doi.org/10.1007/s12649-018-0347-1

Flores, R. A., Urquiaga, S., Alves, B. J. R., Collier, L. S., Zanetti, J. B., & Prado, R. M. (2013). Nitrogen and age on the quality of elephant grass for agroenergy purpose grown in Oxisol. *Semina: Agrarian Sciences*, *34*(1), 127–136. http://doi.org/10.5433/1679-0359.2013v34n1p127

Ghosh, K., Bar, N., Biswas, A. B., & Das, S. K. (2019). Removal of methylene blue (aq) using untreated and acid-treated eucalyptus leaves and GA-ANN modelling. *The Canadian Journal of Chemical Engineering*, *97*(11), 2883–2898. https://doi.org/10.1002/cjce.23503

Gregor, M., Grznár, P., Mozol, Š., & Mozolová, L. (2024). Plackett-Burman design. *Acta Simulation*, *10*(1), 5–9. https://doi.org/10.22306/asim.v10i1.104

Güleç, F., Williams, O., Kostas, E. T., Samson, A., Stevens, L. A., & Lester, E. (2022). A comprehensive comparative study on methylene blue removal from aqueous solution using biochars produced from rapeseed, whitewood, and seaweed via different thermal conversion technologies. *Fuel*, *330*, Article 125428. https://doi.org/10.1016/j.fuel.2022.125428

Imam, T., & Capareda, S. (2012). Characterization of bio-oil, syn-gas and bio-char from switchgrass pyrolysis at various temperatures. *Journal of Analytical and Applied Pyrolysis*, *93*, 170–177. https://doi.org/10.1016/j.jaap.2011.11.010

Irfan, M., Chen, Q., Yue, Y., Pang, R., Lin, Q., Zhao, X., & Chen, H. (2016). Co-production of biochar, bio-oil and syngas from halophyte grass (Achnatherum splendens L.) under three different pyrolysis temperatures. *Bioresource Technology*, *211*, 457–463. https://doi.org/10.1016/j.biortech.2016.03.077

Jawad, A. H., Rashid, R. A., Ishak, M. A. M., Ismail, K. (2018). Adsorptive removal of methylene blue by chemically treated cellulosic waste banana (Musa sapientum) peels . Journal of Taibah University for Science, *12*(6), 809–819. https://doi:10.1080/16583655.2018.1519893

Mateus, N. B., Barbin, D., & Conagin, A. (2001). Feasibility of using the central composition design. *Acta Scientiarum-Tecnologia*, *23*, 1537–1546. https://doi.org/10.4025/actascitechnol.v23i0.2795

Mustapha, O. R., Osobamiro, T. M., Sanyaolu, N. O., & Alabi, O. M. (2023). Adsorption study of Methylene blue dye: an effluents from local textile industry using Pennisteum pupureum (elephant grass). *International Journal of Phytoremediation*, *25*(10), 1348–1358. https://doi.org/10.1080/15226514.2022.2158781

Pedroza, M. M., Machado, P. R. S., Silva, J. G. D, Arruda, M. G., & Picanço, A. P. (2023). Production and application of activated carbon obtained from the thermochemical degradation of corn cob. *Journal of Applied Research and Technology*, *21*(6), 952–964. https://doi.org/10.22201/icat.24486736e.2023.21.6.2173

Pedroza, M. M., Neves, L. H. D., Paz, E. C. S., Silva, F. M., Rezende, C. S. A., Colen, A. G. N., & Arruda, M. G. (2021). Activated charcoal production from tree pruning in the Amazon region of Brazil for the treatment of gray water. *Journal of Applied Research and Technology*, *19*(1), 49–65. https://doi.org/10.22201/icat.24486736e.2021.19.1.1492

Pessoti, B. P. L., Silveira, A. D. M., Moura, R. B., Isidoro, J. M. G. P., Tiezzi, R. O., & Gonçalves, F. A. (2020). Transport of dissolved material on impermeable surface under artificial rainfall analyzed with the application of face-centered experimental design. *Sanitary and Environmental Engineering*, *25*(1), 97–106. https://doi.org/10.1590/S1413-41522020194490

Plackett, R. L., & Burman, J. P. (1946). The design of optimum multifactorial experiments. Biometrika. *Biometrika*, *33*(4), 305–325. https://doi.org/10.1093/biomet/33.4.305

Rodrigues, M. I., & Iemma, A. F. (2014) *Experiment design and process optimization* (3rd ed.). Cárita.

Samson, R., Mani, S., Boddey, R., Sokhansanj, S., Quesada, D., Urquiaga, S., Reis, V., & Holem, C. H. (2005). The potential of C4 perennial grasses for developing a global BIOHEAT industry. *Critical Reviews in Plant Sciences*, *24*(5–6), 461–495. https://doi.org/10.1080/07352680500316508

Silveira Junior, E. G., Silveira, T. C., Perez, V. H., Justo, O. R., David, G. F., & Fernandes, S. A. (2022). Fast pyrolysis of elephant grass: Intensification of levoglucosan yield and other value-added pyrolytic by-products. *Journal of the Energy Institute*, *101*, 254–264. https://doi.org/10.1016/j.joei.2022.02.003

Souza Borges, M. S., Rambo, M. K. D., Duarte, F. A., Burrow, R. A., & Scapin, E. (2025). Remediation of arsenic-contaminated water: high effectiveness of modified biochars from legal amazon residues. *Waste Disposal & Sustainable Energy*, *7*, 381–391. https://doi.org/10.1007/s42768-025-00235-4

Uddin, M., Rahman, M. A., Rukanuzzaman, M., & Islam, M. A. (2017). A potential low cost adsorbent for the removal of cationic dyes from aqueous solutions. *Applied Water Science*, *7*(6), 2831–2842. https://doi:10.1007/s13201-017-0542-4

Wang, K., Peng, N. Zhang, D., Zhou, H., Gu, J., Huang, J., Liu, C., Chen, Y., Liu, Y., & Sun, J. (2023). Efficient removal of methylene blue using Ca(OH)2 modified biochar derived from rice straw. *Environmental Technology & Innovation*, *31*, Article 103145. https://doi.org/10.1016/j.eti.2023.103145

Yusof, M. S. M., Othman, M. H. D., Wahab, R. A., Jumbri, K., Razak, F. I. A., Kurniawan, T. A., Samah, R. A., Mustafa, A., Rahman, M. A., Jaafar, J., & Ismail, A. F. (2020). Arsenic adsorption mechanism on palm oil fuel ash (POFA) powder suspension. *Journal of Hazardous Materials*, *383*, Article 121214. https://doi.org/10.1016/j.jhazmat.2019.121214